



Methylglyoxal-induced mitochondrial dysfunction in vascular smooth muscle cells

Hui Wang, Jianghai Liu, Lingyun Wu*

Department of Pharmacology, College of Medicine, University of Saskatchewan, 107 Wiggins Road, Saskatoon, SK, Canada S7N 5E5

ARTICLE INFO

Article history:

Received 15 January 2009

Accepted 24 February 2009

Keywords:

Methylglyoxal

Mitochondria

Peroxynitrite

Complex III

Alagebrium

ABSTRACT

The effects of methylglyoxal (MG) on mitochondria with specific foci on peroxynitrite (ONOO^-) production, manganese superoxide dismutase (MnSOD) activity, and mitochondrial functions in vascular smooth muscle A-10 cells were investigated. Mitochondrial MG content was significantly increased after A-10 cells were treated with exogenous MG, and so did advanced glycated endproducts (AGEs) formation, indicated by the appearance of N_ϵ -(carboxyethyl) lysine, in A-10 cells. The levels of mitochondrial reactive oxygen species (mtROS) and ONOO^- were significantly increased by MG treatment. Application of ONOO^- specific scavenger uric acid lowered the level of mtROS. MG significantly enhanced the production of mitochondrial superoxide ($\text{O}_2^{\bullet-}$) and nitric oxide (NO), which were inhibited by SOD mimic 4-hydroxy-tempo and mitochondrial nitric oxide synthase (mtNOS) specific inhibitor 7-nitroindazole, respectively. The activity of MnSOD was decreased by MG treatment. Furthermore, MG decreased respiratory complex III activity and ATP synthesis in mitochondria, indicating an impaired mitochondrial respiratory chain. AGEs cross-link breaker alagebrium reversed all aforementioned mitochondrial effects of MG. Our data demonstrated that mitochondrial function is under the control of MG. By inhibiting Complex III activity, MG induces mitochondrial oxidative stress and reduces ATP production. These discoveries will help unmask molecular mechanisms for various MG-induced mitochondrial dysfunction-related cellular disorders.

© 2009 Elsevier Inc. All rights reserved.

1. Introduction

Mitochondria are the powerhouse of mammalian cells. When electrons pass through complexes I–IV of the electron transport chain (ETC), 2–5% of electrons leak out of the ETC and interact with oxygen to form superoxide ($\text{O}_2^{\bullet-}$) in mitochondria, which accounts for about 85% of total intracellular $\text{O}_2^{\bullet-}$ [1,2]. Electron leakage most often occurs at complex I and complex III of the ETC, and the amount of $\text{O}_2^{\bullet-}$ increases dramatically if these complexes are inhibited [3]. Under physiological condition, $\text{O}_2^{\bullet-}$ is converted to hydrogen peroxide (H_2O_2) by manganese superoxide dismutase (MnSOD), which is the primary anti-oxidant defensive enzyme in mitochondria [4]. This anti-oxidant system ensures the clearance of free radicals and protects cells against oxidative damage. Mitochondria also contain specific nitric oxide synthase (mtNOS), which catalyzes the production of nitric oxide (NO) [5]. A considerable amount of NO generated from mtNOS reacts with $\text{O}_2^{\bullet-}$ to form peroxynitrite (ONOO^-) [6]. ONOO^- is a highly reactive

oxidant, damaging proteins, DNA, and lipids [7]. Mitochondrial oxidative stress is tightly related to the pathophysiology of type 2 diabetes and associated complications [8].

Methylglyoxal (MG) is a dicarbonyl compound which readily reacts with certain proteins to form advanced glycated endproducts (AGEs), like *N*-carboxyethyl-lysine (CEL). This rapid interaction contributes to the pathogenesis of insulin resistance syndrome, such as diabetes and hypertension [9–11]. We have previously shown that MG induced the generation of reactive oxygen species (ROS) in hypertensive rat vascular smooth muscle cells (VSMCs) and animal tissues [12,13]. We also found that MG [14] or fructose (a precursor of MG) [15] induced the production of ONOO^- in cultured rat thoracic aortic smooth muscle cells (A-10 cells).

To date, the role of MG in the regulation of mitochondrial function is unclear. We hypothesized that MG affects mitochondrial function by interfering with respiratory complexes and altering mitochondrial ROS production. In the present study, changes in mitochondrial ROS production, activity of mitochondrial complex, and MnSOD activity in A-10 cells in the presence of exogenous MG were investigated. AGEs cross-link breaker alagebrium and non-specific anti-oxidant *n*-acetyl-L-cysteine (NAC) were also used in this study.

* Corresponding author. Tel.: +1 306 966 6310; fax: +1 306 966 6220.

E-mail address: lily.wu@usask.ca (L. Wu).

2. Materials and methods

2.1. Chemicals and antibodies

Anti-nitrotyrosine antibody and bovine serum were purchased from Invitrogen Corporation (Burlington, ON, Canada). Anti-CEL antibody was obtained from Novo Nordisk (A/S, Denmark). Alagebrium was from Alteon Inc. (Parsippany, NJ, USA). Cell culture medium, FITC IgG fluorescent antibody, MG, NAC, o-phenylenediamine (o-PD), 2-methylquinoxaline, 5-methylquinoxaline, KCN, 2,6-dichlorophenolindophenol (DCPIP), rotenone, thenoyltrifluoroacetone (TTFA), antimycin A, coenzyme Q1, cytochrome C, NaN_3 , tween, NADH, decylubiquinol, digitonin, sucrose, MOPS, EDTA, NaPO_3 , fatty acid-free BSA, ATP-free ADP, glutamate and malate were purchased from Sigma–Aldrich (Oakville, ON, Canada).

2.2. Cell culture

A-10 cell, which is a aortic smooth muscle cell line from rats, was obtained from American Type Culture Collection and cultured in Dulbecco's Modified Eagle's Medium (DMEM) containing 10% bovine serum at 37 °C in a humidified atmosphere of 95% air and 5% CO_2 , as described in our previous study [15]. Cells of passages 3–8 were used in this study.

2.3. Isolation of mitochondria

Following the instruction of Mitochondrion Isolation Kit from Sigma–Aldrich (Oakville, ON, Canada), cells were lysed using cell lysis solution (1:150, 5 min) and suspended in extraction buffer A. Unbroken cells and nuclei were pelleted by centrifugation at $600 \times g$ for 10 min. The supernatant was centrifuged at $15,000 \times g$ for 15 min, and the mitochondrial pellet was resuspended in cellytic M cell lysis reagent for MG measurement. The mitochondrial pellet was resuspended in extraction buffer A and freeze–thaw twice for mitochondrial complexes activity determination. Cytochrome C Oxidase Assay Kit from Sigma–Aldrich (Oakville, ON, Canada) was used to determine the integrity of isolated mitochondria. Cytochrome C oxidase is located on the inner mitochondrial membrane and has traditionally been used as a marker for this membrane [16]. The activity of cytochrome C oxidase in isolated mitochondria was high, indicating the high integrity and purity of the preparation.

2.4. MG content determination

MG content was determined using an o-PD method as described previously [15]. In brief, mitochondria isolated from A-10 cells were incubated on ice for 10 min with 1/4 volume of perchloric acid (PCA) and centrifuged (12,000 rpm, 15 min) to remove the PCA-precipitated mitochondrial debris. The supernatant was supplemented with 100 mM o-PD and incubated for 3 h at room temperature. The quinoxaline derivative of MG (2-methylquinoxaline) and the quinoxaline internal standard (5-methylquinoxaline) were measured using a Nova-Pak[®] C18 column (3.9 mm \times 150 mm, and 4 μm particle diameter, MA, USA) equipped with a Hitachi high-performance liquid chromatography (HPLC) system (Hitachi Ltd., Mississauga, ON, Canada).

2.5. Detection of mitochondrial ROS (mtROS) and mitochondrial $\text{O}_2^{\bullet-}$

Mitochondria produce a variety of ROS, such as ONOO^- , NO and $\text{O}_2^{\bullet-}$. MitoTracker Red CM-H₂XROS and MitoSOX from Invitrogen Corporation (Burlington, ON, Canada) were used to detect the levels of mtROS and mitochondrial $\text{O}_2^{\bullet-}$, respectively [17,18]. A-10

cells were seeded on 35 mm glass-bottom dishes and treated with different agents for 18 h. Then, cells were labeled with MitoTracker Red (300 μM , 15 min) or MitoSOX (2 μM , 20 min). After washing, cells were bathed in DMEM again and subjected to examination under a Confocal Laser Scanning Biological Microscope (Olympus Fluoview 300, Olympus America Inc., Melville, NY, USA) coupled with 40 \times objective lens. The exposure time of camera, the gain of amplifier and the aperture were fixed at 4.57 s/scan, 4.0 \times and 3 respectively, to allow quantitative comparisons of the relative fluorescence intensity of the cells between groups. 10–14 cells were randomly collected from 4 different pictures of each groups. The average fluorescence intensity of each cell was measured using Image J program (NIH, USA). Data were expressed as mean \pm SEM of the fluorescence intensity of those cells.

2.6. Measurement of MnSOD activity and NO level

SOD activity of A-10 cells was detected following the instruction of SOD Assay Kit from Cayman Chemical (Ann Arbor, MI, USA). KCN at 3 mM was used to inhibit the activity of Cu/Zn SOD, leaving only MnSOD activity to be measured. For NO detection [15], cells were preloaded with 5 μM membrane-permeable DAF-FM (Invitrogen Corporation, Burlington, ON, Canada) in Krebs' buffer for 2 h at 37 °C. After removal of the excess probe and with different treatments, DAF-fluorescence intensity, reflecting intracellular NO level, was measured with excitation at 495 nm and emission at 515 nm in a Fluoroskan Ascent plate reader (Thermo Labsystem, Helsinki, Finland).

2.7. Immunocytochemistry staining

A-10 cells were seeded on glass cover slips with different treatments for 18 h, and subjected to immuno-staining. As described previously [15], cells were fixed in 4% formalin for 1 h at room temperature. After permeation with 0.1% Triton X-100 for 5 min, fixed cells were incubated with 3% goat serum for 1 h, and then incubated with primary antibody (anti-CEL, 1:100; anti-nitrotyrosine, 1:200) at 4 °C overnight. Cells were washed in PBS (0.01 M) for 15 min and incubated with diluted fluorescent secondary antibody (FITC-IgG, 1:200) for 3 h at room temperature. After washed with PBS, cells were mounted on glass slides and observed under a *confocal microscope*. Fluorescence intensity was measured using Image J program.

2.8. Detection of the activities of complex I, complex III, and complex IV

Mitochondrial complex I activity was determined by monitoring the reduction of DCPIP at 600 nm with the addition of assay buffer (10 \times buffer containing 0.5 M Tris–HCl at pH 8.1, 1% BSA, 10 μM antimycin A, 3 mM KCN, 0.5 mM coenzyme Q₁) [19]. Mitochondrial proteins (25 $\mu\text{g}/\text{ml}$) and DCPIP (64 μM) were added to the assay buffer before using. The reaction was started by adding 200 μM NADH and scanned at 600 nm with the reference wavelength of 620 nm for 2 min. Mitochondrial complex III activity was detected by monitoring the reduction of cytochrome C at 550 nm upon the addition of assay buffer (10 \times buffer contains 0.5 M Tris–HCl at pH 7.8, 2 mM NaN_3 , 0.8% Tween-20, 1% BSA, 2 mM decylubiquinol) with 40 μM cytochrome C [19]. The reaction was started by adding 20 $\mu\text{g}/\text{ml}$ mitochondria proteins to the assay buffer and scanned at 550 nm with the reference wavelength of 540 nm for 2 min. Mitochondrial complex IV activity was measured by monitoring the reduction of reduced cytochrome C at 550 nm with the addition of assay buffer (0.5 M phosphate buffer at pH 8.0, 1% BSA and 2% tween) [19]. Freshly prepared reduced cytochrome C (80 μM) was added to the assay

buffer before using. The reaction was started by adding mitochondria protein (20 $\mu\text{g}/\text{ml}$) and scanned at 550 nm with the reference wavelength of 540 nm for 2 min. All assays were performed at 37 °C.

2.9. Determination of ATP synthesis

ATP synthesis was assayed based on a modified method of Atorino et al. [20]. Briefly, cells were incubated at 37 °C for 30 min in a respiratory buffer (0.02% digitonin, 0.25 M sucrose, 20 mM MOPS, 1 mM EDTA, 5 mM NaPO_3 , 0.1% fatty acid-free BSA, 1 mM ATP-free ADP, 5 mM glutamate, and 5 mM malate, pH 7.4). Thereafter, 3% PCA was used to precipitate proteins, and samples were centrifuged at 13,000 rpm for 2 min. Supernatants were taken out to measure ATP after pH adjusted to 7.8 using 10 M KOH. ATP was detected using ATP Bioluminescent Assay Kit from Sigma–Aldrich (Oakville, ON, Canada). Data were expressed as nanomoles of ATP per milligram of protein.

2.10. Statistical analysis

Data were expressed as mean \pm SEM from at least three independent experiments. Statistical analysis was performed by one-way analysis of variance (ANOVA). Differences between groups were examined by Student's unpaired *t*-Test. Values are considered to be statistically significant when $p < 0.05$.

3. Results

3.1. Effect of MG on mtROS generation

After A-10 cells were treated with exogenous MG (30 μM) for 18 h, mitochondrial MG content increased by 50.7% (0.205 ± 0.012

nmol/mg vs. 0.136 ± 0.014 nmol/mg mitochondrial protein, $p < 0.01$, $n = 4$ for each group). Alagebrium (50 μM) had no effect on basal content of mitochondrial MG but its presence decreased the effect of exogenous MG on mitochondrial MG content (0.14 ± 0.009 nmol/mg vs. 0.205 ± 0.01 nmol/mg mitochondrial protein, $p < 0.01$, $n = 4$ for each group). NAC (600 μM) had no effect on mitochondrial MG content.

MG increased the fluorescence intensity of CEL in a concentration-dependent manner. At 30 μM , MG increased the fluorescence intensity of CEL by 321% (Fig. 1A and B). Co-treatment with alagebrium (50 and 100 μM) decreased the effect of 30 μM MG (Fig. 1A and C). NAC (600 μM) did not show any effect on the staining of CEL (data not shown).

Exposure of cells to MG (5–100 μM) caused a significant concentration-dependent increase in mtROS generation. The production of mtROS increased dramatically with 30 μM MG and reached a plateau with 100 μM MG (Fig. 2A and B). Co-incubation of NAC (600 μM) significantly decreased mtROS generation induced by MG (Fig. 2A and B). Alagebrium (50 and 100 μM) and ONOO[−] specific scavenger uric acid (50 μM) inhibited mtROS generation induced by 30 μM MG (Fig. 2A, C and D).

3.2. Effects of MG on NO and nitrotyrosine generation

The effect of MG on NO generation was evaluated by DAF-FM, a specific probe used for quantitating low concentration of NO. As shown in Fig. 3, MG (30 μM) increased the production of NO by 48% ($p < 0.01$). Alagebrium (50 μM), NAC (600 μM), and mtNOS inhibitor 7-nitroindazole (50 μM) significantly reduced MG-increased NO generation.

Nitrotyrosine is formed by ONOO[−]-mediated nitration of tyrosine residues of proteins. As shown in Fig. 4A and C, MG (20 and 30 μM) significantly increased the fluorescence intensity of

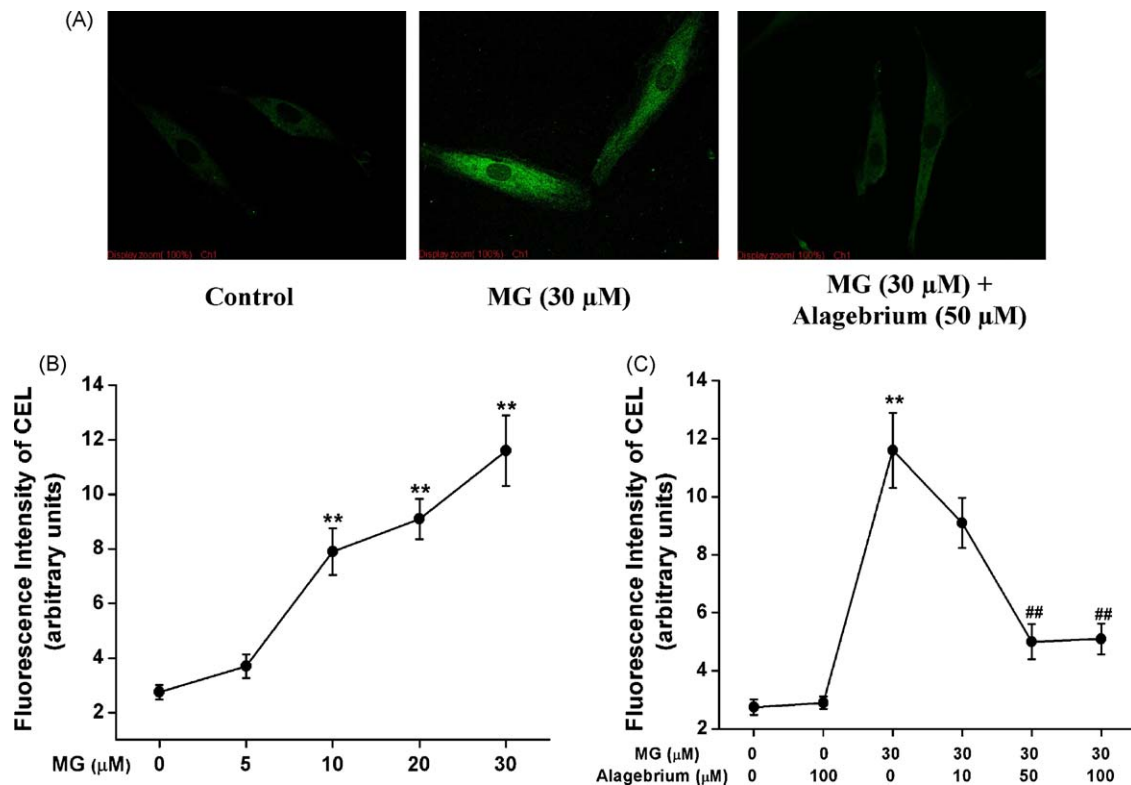


Fig. 1. Effect of MG on the fluorescence intensity of CEL in A-10 cells. (A) MG increased the staining of CEL in A-10 cells, which was decreased by alagebrium. (B) Cells were treated with MG (5–30 μM). (C) Cells were co-treated with alagebrium (10–100 μM) and MG (30 μM). After treated with different agents for 18 h, cells were stained using anti-CEL (1:100 at 4 °C overnight) and secondary fluorescent antibody (FITC-IgG, 1:200 at room temperature for 3 h) and read under Confocal microscope. Fluorescence intensity was analyzed using Image J program. ** $p < 0.01$ vs. cells without any treatment; ## $p < 0.01$ vs. cells treated with MG (30 μM) alone. $n = 12$.

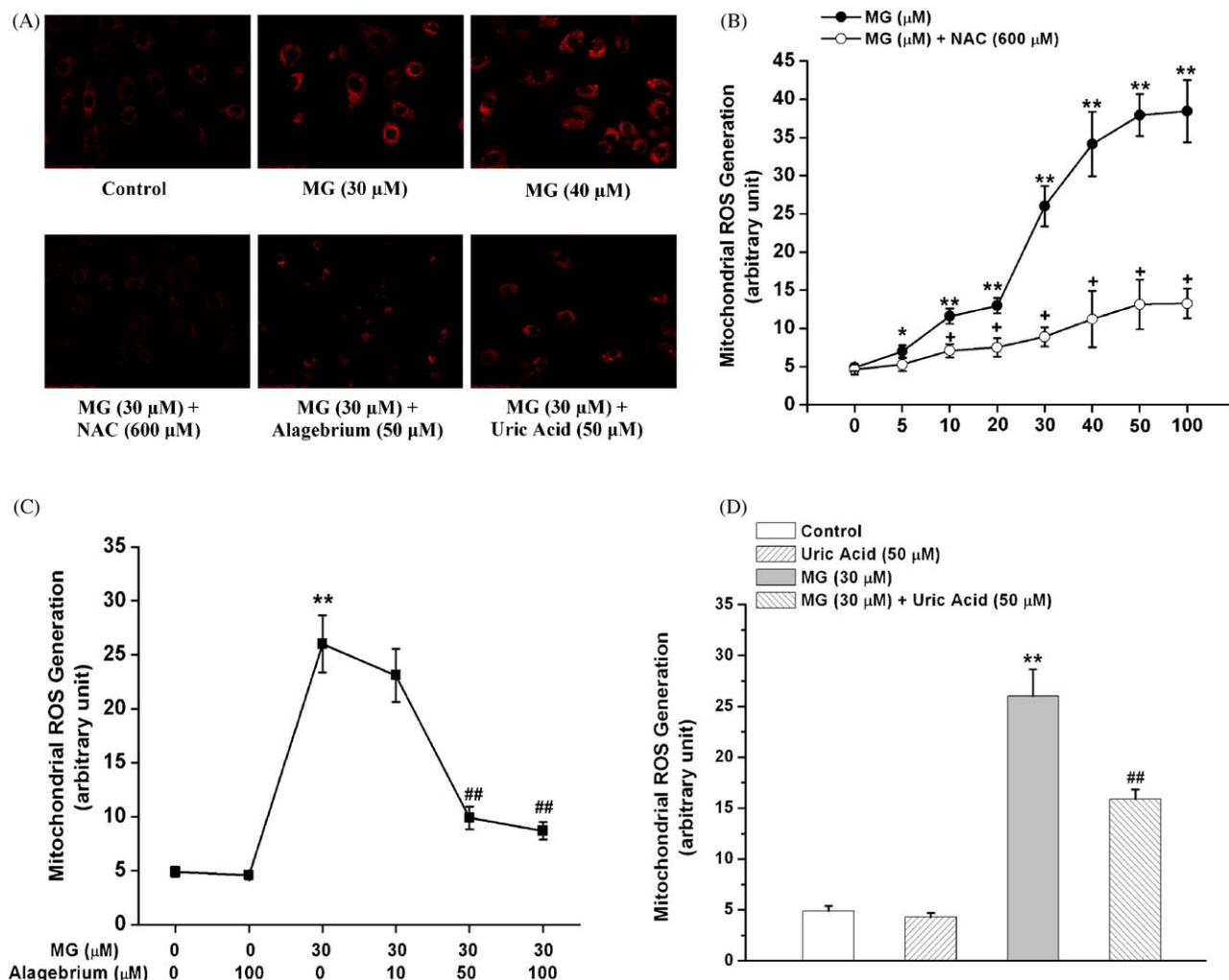


Fig. 2. Effect of MG on mitochondrial ROS generation in A-10 cells. (A) MG-enhanced mitochondrial ROS generation, which was decreased by *n*-acetyl-L-cysteine (NAC), alagebrium, and uric acid. (B) Cells were treated with MG (5–100 μ M) in the presence or absence of NAC (600 μ M). (C) Cells were co-treated with alagebrium (10–100 μ M) and MG (30 μ M). (D) Cells were co-treated with uric acid (50 μ M) and MG (30 μ M). After 18 h treatment with different agents, cells were loaded with molecular probe MitoTracker Red (300 μ M, 15 min) and read under Confocal microscope. Fluorescence intensity was analyzed using Image J program. * $p < 0.05$ and ** $p < 0.01$ vs. cells without any treatment; + $p < 0.01$ vs. MG treatment alone at the same concentration; ## $p < 0.01$ vs. cells treated with MG (30 μ M) alone. $n = 10$ –14.

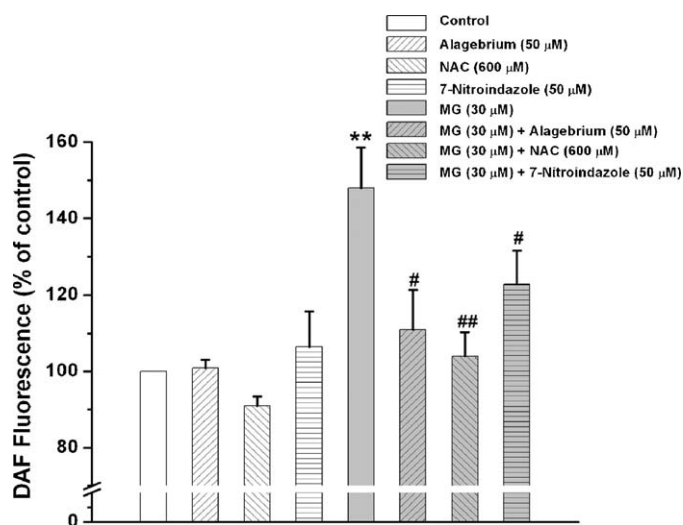


Fig. 3. Effect of MG on NO production in A-10 cells. Cells were treated with different agents for 18 h. Molecular probe DAF-FM (5 μ M, 2 h) was used to detect cellular levels of NO. ** $p < 0.01$ vs. control; # $p < 0.05$ and ## $p < 0.01$ vs. cells treated with MG (30 μ M) alone. $n = 8$. NAC, *n*-acetyl-L-cysteine.

nitrotyrosine in A-10 cells by 176–191%. The addition of NAC (600 μ M) significantly inhibited the formation of nitrotyrosine induced by MG. Co-incubation of alagebrium (50 μ M) also significantly reduced the fluorescence intensity of nitrotyrosine induced by MG (30 μ M) (Fig. 4A and D). Nitrotyrosine and mitotracker were co-localized in the tested cells as indicated by the overlap of yellow and red-green images (Fig. 4B).

3.3. Effect of MG on mitochondrial $O_2^{\bullet-}$ generation

MitoSOX, a specific probe to detect mitochondrial $O_2^{\bullet-}$ level, was used in this assay. MG (30 μ M) increased mitochondrial $O_2^{\bullet-}$ production by 69.9% ($p < 0.01$), compared with untreated cells. Co-incubation of alagebrium (50 μ M) and SOD mimic 4-hydroxy-tempo (Tempo, 500 μ M) decreased mitochondrial $O_2^{\bullet-}$ production induced by MG treatment by 57% ($p < 0.01$) and 85.8% ($p < 0.01$), respectively (Fig. 5A and B).

3.4. Effect of MG on MnSOD activity

MG (5–30 μ M) decreased the activity of MnSOD, the first line enzyme to scavenge $O_2^{\bullet-}$ in mitochondria. MG at 30 μ M decreased MnSOD activity by 24.5% ($p < 0.05$)

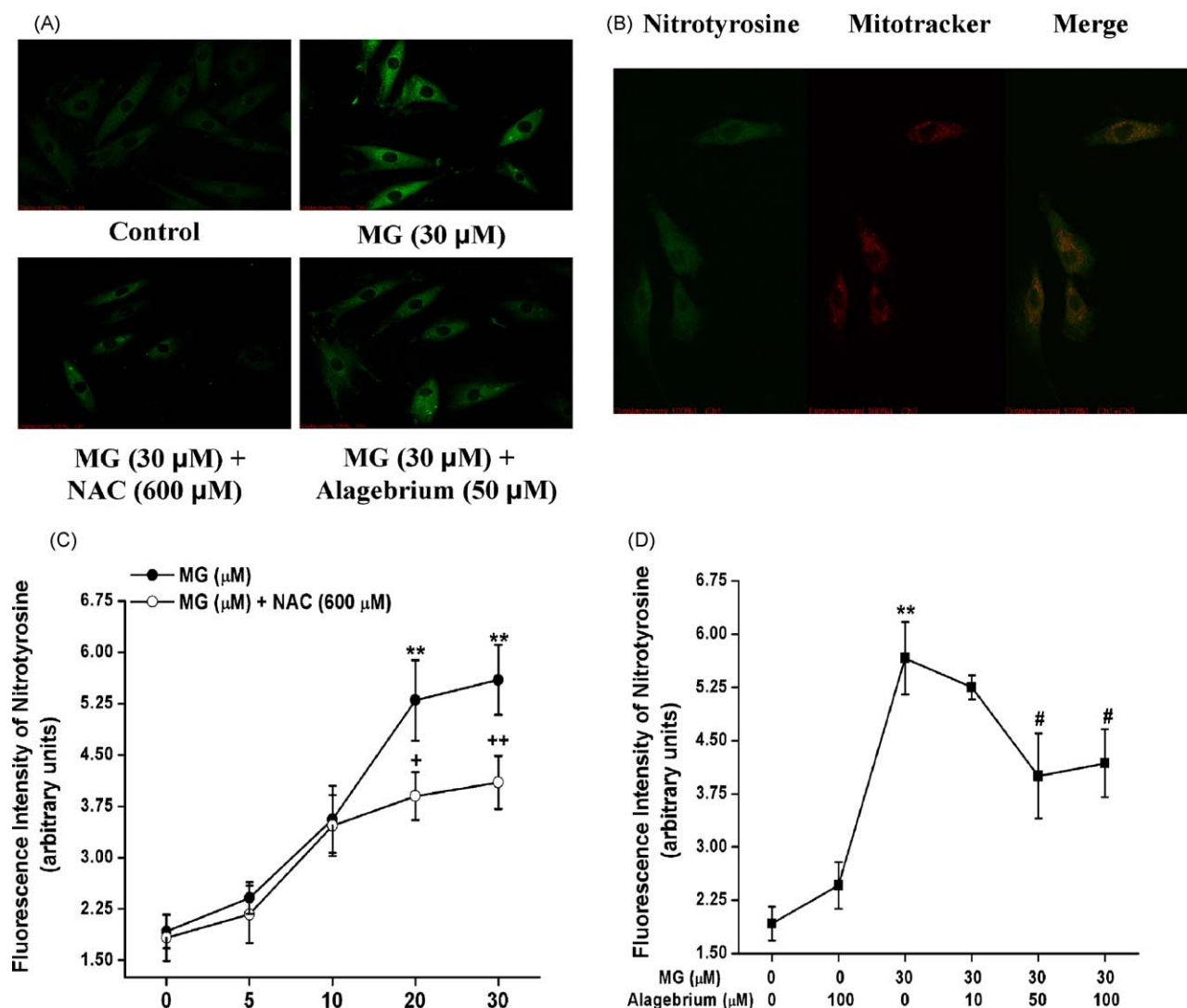


Fig. 4. Effect of MG on the fluorescence intensity of nitrotyrosine in A-10 cells. (A) MG increased nitrotyrosine staining, which was inhibited by alagebrium and *n*-acetyl-L-cysteine (NAC). (B) Cells were co-stained with anti-nitrotyrosine and MitoTracker Red to determine whether increased nitrotyrosine was located in mitochondria. (C) Cells were treated with MG (5–30 μ M) in the presence or absence of NAC (600 μ M). (D) Cells were co-treated with alagebrium (10–100 μ M) and MG (30 μ M). Cells were treated with different agents for 18 h. Double cell staining of MitoTracker Red (300 μ M, 15 min) and nitrotyrosine (anti-nitrotyrosine 1:200 at 4 °C overnight; FITC-IgG 1:200 at room temperature for 3 h) were conducted. Cells were read under Confocal microscope. Fluorescence intensity was measured using Image J program. ** $p < 0.01$ vs. cells without any treatment; + $p < 0.05$ and ++ $p < 0.01$ vs. MG treatment alone at the same concentration; # $p < 0.05$ vs. cells treated with MG (30 μ M) alone. $n = 10$ –14.

(Fig. 6A). Alagebrium (10–100 μ M) normalized MG-decreased MnSOD activity (Fig. 6B). NAC (600 μ M) had no effect on MnSOD activity (data not shown).

3.5. Effect of MG on mitochondrial functions

MG (30 μ M) treatment for 18 h had no obvious effect on the activity of complex I or complex IV, but significantly decreased complex III activity by 11.7% ($p < 0.05$), as shown in Fig. 7A. Alagebrium (50 μ M) inhibited the effect of MG on complex III by 64.61% ($p < 0.05$). NAC (600 μ M) did not have effect on complex III activity (data not shown).

In order to confirm the effect of MG on mitochondrial ETC complexes, complex inhibitors were used to treat cells for 2 h in the absence or presence of MG. Mitochondrial $O_2^{\bullet-}$ generation was thereafter determined using the specific probe MitoSOX. Rotenone (0.5 and 1 μ M), TTFA (5 and 10 μ M), antimycin A (3 and 5 μ M) and KCN (0.5 and 1 mM), which are respective blockers of complex I, complex II, complex III and Complex IV, significantly increased production of mitochondrial $O_2^{\bullet-}$ in A-10 cells (Fig. 7B). No

difference was observed between effects of two concentrations of each blocker. Therefore, these inhibitors appear to maximally inhibit the respective complexes. Interestingly, MG (30 μ M) further increased rotenone (1 μ M), TTFA (10 μ M) and KCN (1 mM)-induced mitochondrial $O_2^{\bullet-}$ generation by 48.11%, 52.6% and 40.2%, respectively, in comparison with the cells treated with the inhibitor alone. However, the addition of MG (30 μ M) did not change complex III inhibitor (antimycin A)-induced mitochondrial $O_2^{\bullet-}$ generation. These results suggested that MG targeted on complex III to induce mitochondrial $O_2^{\bullet-}$ generation (Fig. 7B). MG (30 μ M) significantly lowered ATP production by 44.8% (4.76 ± 0.74 nmol/mg vs. 8.62 ± 0.24 nmol/mg protein, $p < 0.01$). Alagebrium (50 μ M) restored ATP synthesis inhibited by MG by 78.0% (Fig. 8).

4. Discussion

MG causes cross-link among lysine, cysteine, and arginine residues of selective proteins to form AGEs, like CEL, altering the structure of proteins and their functions [9]. Higher levels of MG

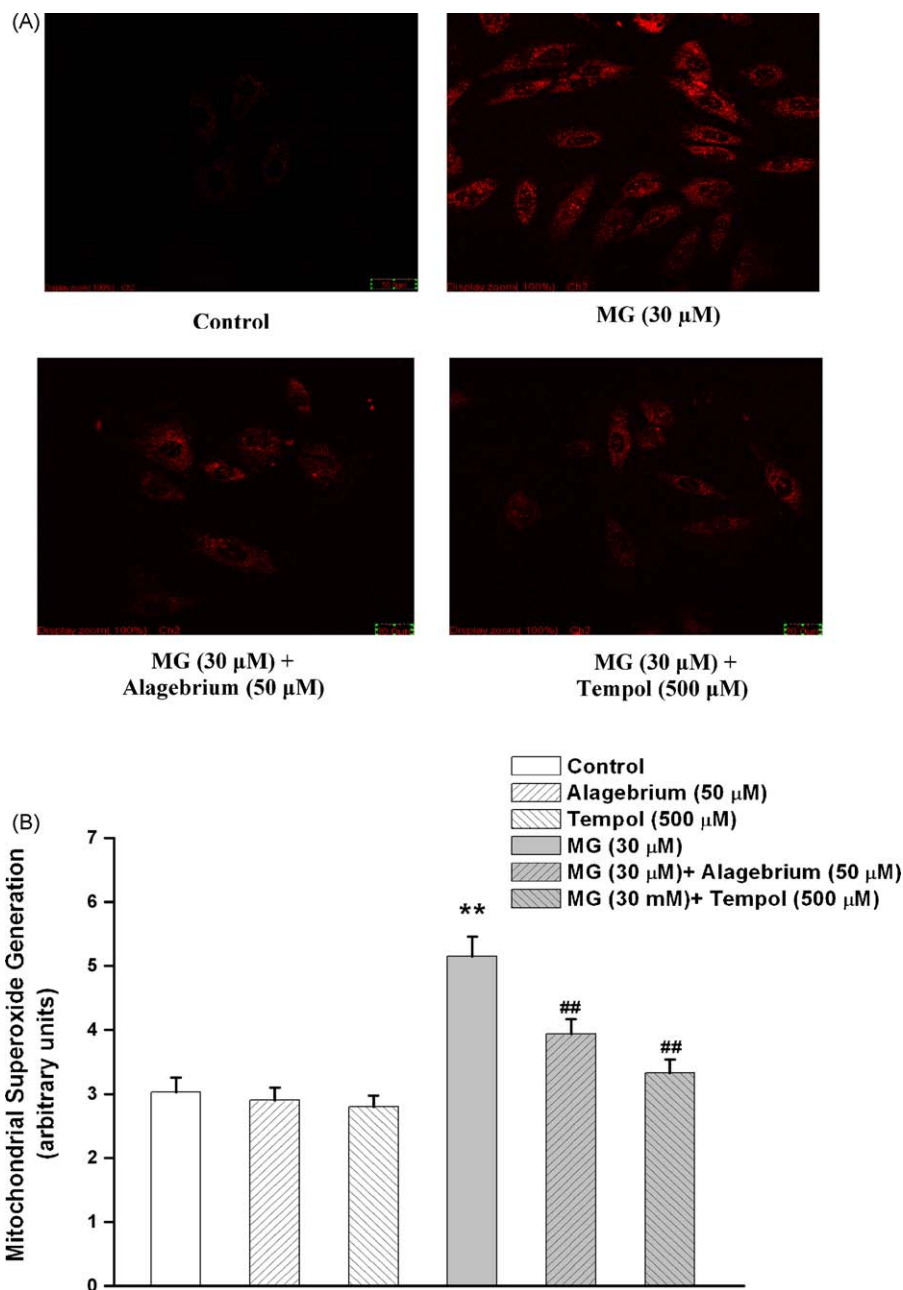


Fig. 5. Effect of MG on mitochondrial $O_2^{\bullet-}$ generation in A-10 cells. (A) MG increased MitoSOX signal in mitochondria, which was decreased by alagebrium and 4-hydroxy-tempo (Tempol). (B) Mitochondrial $O_2^{\bullet-}$ generation in A-10 cells. After treated with different agents for 18 h, cells were loaded with molecular probe MitoSOX (2 μ M, 20 min) and read under Confocal microscope. Fluorescence intensity was measured using ImageJ program. ** $p < 0.01$ vs. control; ## $p < 0.01$ vs. cells treated with MG (30 μ M) alone. $n = 12$.

have been found in diabetic patients than in healthy controls [21]. In the present study, we observed that mitochondrial MG content was significantly increased after the cells were treated with exogenous MG. It appears that MG can move across plasmalemma and mitochondrial membrane to attack different molecular targets. Once inside the cells, MG induces glycation of many proteins in the cytosol, mitochondria and other vesicles. The formation of CEL in mitochondria may result in the dysfunction of mitochondrial proteins, and furthermore, increase mtROS generation. Alagebrium, an AGEs cross-link breaker [22], not only decreased CEL formation, but also diminished MG levels in mitochondria. The result indicates that alagebrium scavenges MG and inhibits glycation directly, although the mechanism is unknown. This discovery also echoes the observation obtained by Nobecourt et al. [23].

The physiological concentration of plasma MG in rats is approximately 5 μ M [24]. Our previous study detected the plasma MG levels of 33.6 μ M in 20-week-old SHR and 14.2 μ M in age-matched WKY rats [25]. Plasma levels of MG increased from 3.3 μ M in healthy humans to 5.9 μ M in type 2 diabetic patients [21]. In addition, cultured cells may produce more MG since MG concentration up to 310 μ M was detected in cultured Chinese hamster ovary cells [26]. Furthermore, up to 10 mM MG had been used to investigate its effect on insulin secreting cells and insulin signaling pathways in rat L6 myoblasts [27,28]. Thus, MG (30 μ M) used in the present study is not only the physiological relevant concentration, but also suitable to mimic the insulin resistance environment in rat aortic smooth muscle cells.

Our previous work has shown that MG induced overproduction of $O_2^{\bullet-}$, NO, and ONOO $^-$ in rat VSMCs [14]. The present study

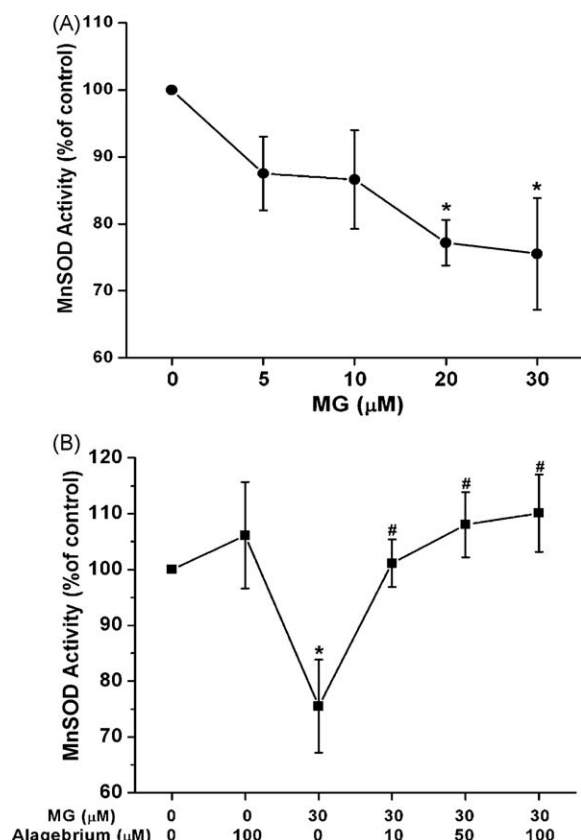


Fig. 6. Effect of MG on MnSOD activity in A-10 cells. (A) MG (5–30 μ M) decreased MnSOD activity in A-10 cells. (B) MnSOD activity in A-10 cells co-treated with alagebrium (10–100 μ M) and MG (30 μ M). Cells were treated with different agents for 18 h. SOD Assay Kit was used to detect SOD activity. KCN at 3 mM was used to inhibit the activity of Cu/Zn SOD, leaving only MnSOD activity to be measured. * $p < 0.05$ vs. cells without any treatment; # $p < 0.05$ vs. cells treated with MG (30 μ M) alone. $n = 4$.

demonstrated that mitochondria are targets of MG for this pro-oxidative action. More specifically, we demonstrated that MG increased mitochondrial ONOO⁻ production in VSMCs. Several lines of evidence support this conclusion. (1) Uric acid, a specific scavenger of ONOO⁻, significantly decreased MG-induced mtROS generation. (2) Increased staining of nitrotyrosine was observed in MG treated A-10 cells, and the expression of nitrotyrosine was mostly co-localized with mitochondrial marker staining. (3) MnSOD is the major enzyme which catalyzes O₂^{•-} degradation in mitochondria and protects mitochondria against oxidative stress. Our results show that MG reduced the activity of MnSOD in mitochondria of VSMCs. (4) MG-induced mitochondrial O₂^{•-} production was inhibited by Tempol. As a SOD mimic, Tempol is more stable and membrane-permeable than MnSOD itself [29]. (5) Located on the inner mitochondrial membrane, mtNOS is considered as the alpha-isoform of neuronal nitric oxide synthase (nNOS) and is responsible for NO production in mitochondria [30,31]. MG-induced intracellular NO was decreased by 7-nitroindazole. The latter is the specific inhibitor of mtNOS [32] and can prevent mitochondrial structural damage mediated by increased mitochondria NO generation in the developing brain [33]. Together with MG-induced mitochondrial O₂^{•-}, the stimulation of mtNOS by MG also contributes to ONOO⁻ formation.

Of particular importance is our observation that MG selectively damaged complex III activity, not complex I or complex IV. This effect may underlie MG-inhibited ATP synthesis and MG-enhanced ROS production. Further evidence for the inhibition of complex III by MG was derived from the failure of MG to

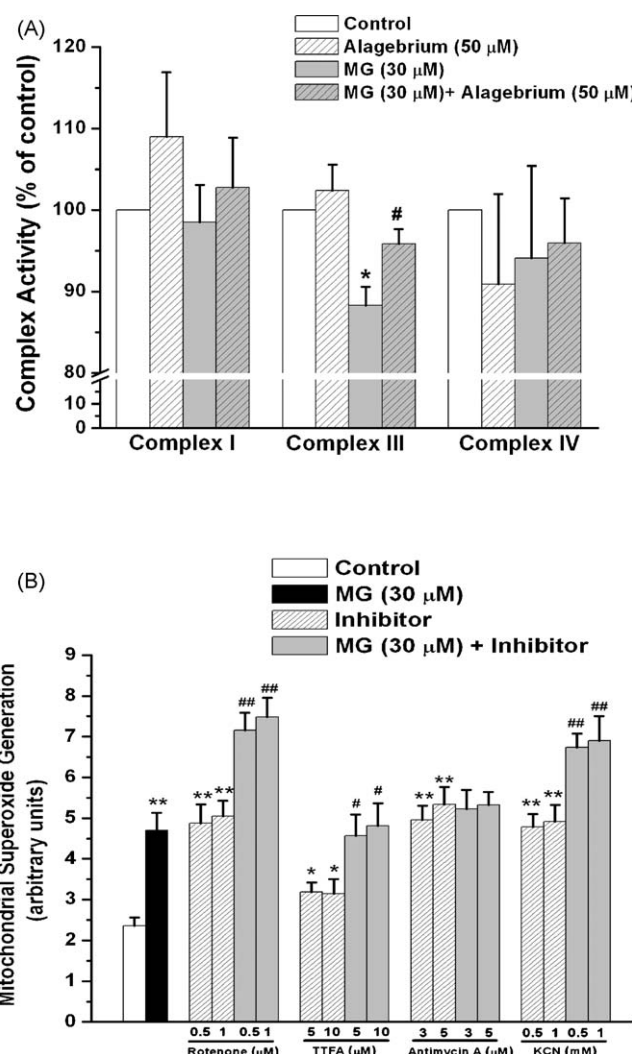


Fig. 7. Effect of MG on mitochondrial complexes in A-10 cells. (A) Effect of MG on activities of complex I, complex III and complex IV in A-10 cells. Cells were treated with different agents for 18 h. * $p < 0.05$ vs. control; # $p < 0.05$ vs. cells treated with MG (30 μ M) alone. $n = 4$. (B) Effect of MG on mitochondrial O₂^{•-} generation in the presence of different inhibitors of respiratory complexes. A-10 cells were treated with different agents for 2 h. Rotenone, thenoyltrifluoroacetone (TTFA), antimycin A and KCN are inhibitors of complexes I, II, III and IV, respectively. * $p < 0.05$ and ** $p < 0.01$ vs. control; # $p < 0.05$ and ## $p < 0.01$ vs. inhibitor alone treated cells. $n = 12$.

increase mitochondria O₂^{•-} generation in the presence of antimycin A, a specific blocker of complex III. That alagebrium restored MG-inhibited complex III activity suggests that the complex III is glycosylated by MG. Complex III, which is also called cytochrome C reductase, transfers electrons from ubiquinone to cytochrome C. The inhibition of complex III by MG may disrupt the ETC, rendering more electrons leaking out to form O₂^{•-}. Consequently, hydrogen electrochemical gradient across the inner mitochondrial membrane is weakened, and the driving force for ATPase to synthesize ATP provided by hydrogen influx across the inner mitochondrial membrane is reduced. Cellular integrity and function are therefore compromised. Although we did not directly measure the activity of complex II in the presence of MG, our experiments with complex II inhibitor, TTFA, indicate that complex II is not a major site of mitochondrial O₂^{•-} generation in A-10 cells. Furthermore, after complex II is maximally inhibited by TTFA, MG still induced mitochondrial O₂^{•-} production. This shows that the effect of MG on superoxide production does not depend on complex II. Evidence shows that

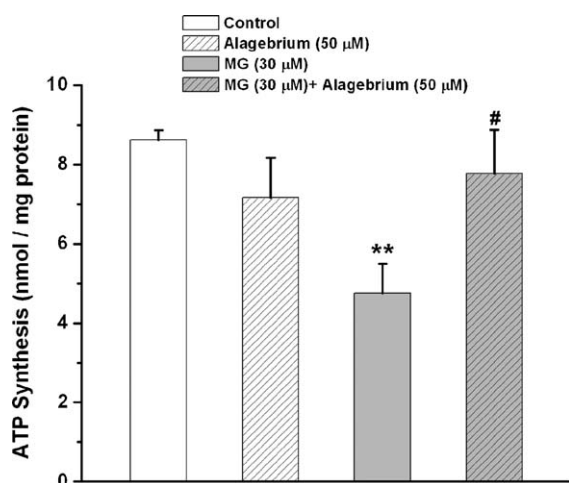


Fig. 8. Effect of MG on ATP synthesis (30 min) in mitochondria of A-10 cells. Cells were treated with different agents for 18 h, and ATP levels were determined using ATP Bioluminescent Assay Kit. ** $p < 0.01$ vs. control; # $p < 0.05$ vs. cells treated with MG (30 μM) alone. $n = 4$.

mitochondrial dysfunction, especially elevated production of mtROS resulted from Complex III inhibition, is closely linked with the pathogenesis of insulin resistance [8]. Moreover, normalization of mitochondrial superoxide production blocked the diabetic hyperglycemia damage in bovine aortic endothelial cells [34]. Therefore, complex III dysfunction-induced mitochondrial oxidative stress plays an important role in the pathophysiology of insulin resistance syndrome.

In addition, our study demonstrated that alagebrium reversed all harmful effects of MG on mitochondria of cultured cells. Compared with alagebrium, the beneficial effect of NAC is limited. It reduced MG-induced ROS, NO, and nitrotyrosine production, but did not affect mitochondrial functions.

In summary, our study demonstrates that MG plays a critical role in regulating mitochondrial functions of VSMC. Respiratory complex III is the major and selective target of MG in mitochondria. Together with reduced MnSOD activity and disruption of the ETC in the presence of MG largely explain the increased oxidative stress and decreased ATP production in many MG-related cellular disorders. These novel observations provide new inside in the physiological importance and pathophysiological implications of the interaction of MG with mitochondria functions. It also sheds light on pathogenesis of and treatment for many mitochondrial-originated cellular disorders encountered in insulin resistance syndrome.

Acknowledgements

This work was supported by operating grants from the Canadian Institutes of Health Research (CIHR, MOP-68938) and from Heart and Stroke Foundation of Saskatchewan to L. Wu. H. Wang is supported by a studentship from the GREAT program of CIHR/Heart and Stroke Foundation of Canada.

References

- [1] Chance B, Oshino N, Sugano T, Mayevsky A. Basic principles of tissue oxygen determination from mitochondrial signals. *Adv Exp Med Biol* 1973;37A:277–92.
- [2] Droge W. Free radicals in the physiological control of cell function. *Physiol Rev* 2002;82:47–95.
- [3] Turrens JF. Mitochondrial formation of reactive oxygen species. *J Physiol* 2003;552:335–44.
- [4] Li M, Chiu JF, Mossman BT, Fukagawa NK. Down-regulation of manganese-superoxide dismutase through phosphorylation of FOXO3a by Akt in explanted vascular smooth muscle cells from old rats. *J Biol Chem* 2006;281:40429–3.

- [5] Epperly MW, Cao S, Zhang X, Francicola D, Shen H, Greenberger EE, et al. Increased longevity of hematopoiesis in continuous bone marrow cultures derived from NOS1 (nNOS, mtNOS) homozygous recombinant negative mice correlates with radioresistance of hematopoietic and marrow stromal cells. *Exp Hematol* 2007;35:137–45.
- [6] Dedkova EN, Ji X, Lipsius SL, Blatter LA. Mitochondrial calcium uptake stimulates nitric oxide production in mitochondria of bovine vascular endothelial cells. *Am J Physiol Cell Physiol* 2004;286:C406–15.
- [7] Valko M, Leibfriz D, Moncol J, Cronin MT, Mazur M, Telser J. Free radicals and antioxidants in normal physiological functions and human disease. *Int J Biochem Cell Biol* 2007;39:44–84.
- [8] Kim JA, Wei Y, Sowers JR. Role of mitochondrial dysfunction in insulin resistance. *Circ Res* 2008;102:401–14.
- [9] Wang X, Jia X, Chang T, Desai K, Wu L. Attenuation of hypertension development by scavenging methylglyoxal in fructose-treated rats. *J Hypertens* 2008;26:765–72.
- [10] Goh SY, Cooper ME. The role of advanced glycation end products in progression and complications of diabetes. *J Clin Endocrinol Metab* 2008;93:1143–52.
- [11] Jia X, Olson DJ, Ross AR, Wu L. Structural and functional changes in human insulin induced by methylglyoxal. *FASEB J* 2006;20:1555–7.
- [12] Wu L, Juurlink BH. Increased methylglyoxal and oxidative stress in hypertensive rat vascular smooth muscle cells. *Hypertension* 2002;39:809–14.
- [13] Desai KM, Wu L. Free radical generation by methylglyoxal in tissues. *Drug Metab Drug Interact* 2008;23:151.
- [14] Chang T, Wang R, Wu L. Methylglyoxal-induced nitric oxide and peroxynitrite production in vascular smooth muscle cells. *Free Radic Biol Med* 2005;38:286–93.
- [15] Wang H, Meng QH, Chang T, Wu L. Fructose-induced peroxynitrite production is mediated by methylglyoxal in vascular smooth muscle cells. *Life Sci* 2006;79:2448–54.
- [16] Duan S, Hajek P, Lin C, Shin SK, Attardi G, Chomyn A. Mitochondrial outer membrane permeability change and hypersensitivity to digitonin early in staurosporine-induced apoptosis. *J Biol Chem* 2003;278:1346–53.
- [17] Busik JV, Mohr S, Grant MB. Hyperglycemia-induced reactive oxygen species toxicity to endothelial cells is dependent on paracrine mediators. *Diabetes* 2008.
- [18] Schroeder P, Pohl C, Calles C, Marks C, Wild S, Krutmann J. Cellular response to infrared radiation involves retrograde mitochondrial signaling. *Free Radic Biol Med* 2007;43:128–35.
- [19] Long J, Wang X, Gao H, Liu Z, Liu C, Miao M, et al. Malonaldehyde acts as a mitochondrial toxin: inhibitory effects on respiratory function and enzyme activities in isolated rat liver mitochondria. *Life Sci* 2006;79:1466–72.
- [20] Atorino L, Silvestri L, Koppen M, Cassina L, Ballabio A, Marconi R, et al. Loss of m-AAA protease in mitochondria causes complex I deficiency and increased sensitivity to oxidative stress in hereditary spastic paraplegia. *J Cell Biol* 2003;163:777–87.
- [21] Wang H, Meng QH, Gordon JR, Khandwala H, Wu L. Proinflammatory and proapoptotic effects of methylglyoxal on neutrophils from patients with type 2 diabetes mellitus. *Clin Biochem* 2007;40:1232–9.
- [22] Desai K, Wu L. Methylglyoxal and advanced glycation endproducts: new therapeutic horizons? *Recent Patents Cardiovasc Drug Discov* 2007;2:89–99.
- [23] Nobecourt E, Zeng J, Davies MJ, Brown BE, Yadav S, Barter PJ, et al. Effects of cross-link breakers, glycation inhibitors and insulin sensitizers on HDL function and the non-enzymatic glycation of apolipoprotein A-I. *Diabetologia* 2008;51:1008–17.
- [24] Nagaraj RH, Sarkar P, Mally A, Biemel KM, Lederer MO, Padayatti PS. Effect of pyridoxamine on chemical modification of proteins by carbonyls in diabetic rats: characterization of a major product from the reaction of pyridoxamine and methylglyoxal. *Arch Biochem Biophys* 2002;402:110–9.
- [25] Wang X, Desai K, Clausen JT, Wu L. Increased methylglyoxal and advanced glycation end products in kidney from spontaneously hypertensive rats. *Kidney Int* 2004;66:2315–21.
- [26] Chaplin FW, Fahl WE, Cameron DC. Evidence of high levels of methylglyoxal in cultured Chinese hamster ovary cells. *Proc Natl Acad Sci USA* 1998;95:5533–8.
- [27] Shearer EA, Benson RS, Best L. Cytotoxic action of methylglyoxal on insulin-secreting cells. *Biochem Pharmacol* 2001;61:1381.
- [28] Riboulet-Chavey A, Pierron A, Durand I, Murdaca J, Giudicelli J, Van Obberghen E. Methylglyoxal impairs the insulin signaling pathways independently of the formation of intracellular reactive oxygen species. *Diabetes* 2006;55:1289–99.
- [29] Chatterjee PK, Cuzzocrea S, Brown PA, Zacharowski K, Stewart KN, Mota-Filipe H, et al. Tempol, a membrane-permeable radical scavenger, reduces oxidant stress-mediated renal dysfunction and injury in the rat. *Kidney Int* 2000;58:658–73.
- [30] Kanai AJ, Pearce LL, Clemens PR, Birdier LA, VanBibber MM, Choi SY, et al. Identification of a neuronal nitric oxide synthase in isolated cardiac mitochondria using electrochemical detection. *Proc Natl Acad Sci USA* 2001;98:14126–31.
- [31] Elfering SL, Sarkela TM, Giulivi C. Biochemistry of mitochondrial nitric-oxide synthase. *J Biol Chem* 2002;277:38079–86.
- [32] Carreras MC, Melani M, Riobo N, Converso DP, Gatto EM, Poderoso JJ. Neuronal nitric oxide synthases in brain and extraneural tissues. *Methods Enzymol* 2002;359:413–23.
- [33] Giusti S, Converso DP, Poderoso JJ, Fiszer de Plazas S. Hypoxia induces complex I inhibition and ultrastructural damage by increasing mitochondrial nitric oxide in developing CNS. *Eur J Neurosci* 2008;27:123–31.
- [34] Nishikawa T, Edelstein D, Du XL, Yamagishi S, Matsumura T, Kaneda Y, et al. Normalizing mitochondrial superoxide production blocks three pathways of hyperglycaemic damage. *Nature* 2000;404:787–90.